Novel Acetylene-Terminated Polyisoimides with Excellent Processability and Properties Comparison with Corresponding Polyimides

Heng Zhou,[1,2] Feng Liu,[1] Yongsheng Zhang,[1] Weifeng Fan,[3] Jingfeng Liu,[3] Zhen Wang,[3] Tong Zhao[1]

[1]*High Technology Materials Laboratory, Institute of Chemistry, Chinese Academy of Sciences, Beijing 100190, People's Republic of China*
[2]*Graduate University of Chinese Academy of Sciences, Beijing 100049, People's Republic of China*
[3]*State Key Laboratory of Polymer Physics and Chemistry, Changchun Institute of Applied Chemistry, Chinese Academy of Sciences, Changchun 130022, People's Republic of China*

Received 15 April 2011; accepted 19 April 2011
DOI 10.1002/app.34718
Published online 17 August 2011 in Wiley Online Library (wileyonlinelibrary.com).

ABSTRACT: Two novel acetylene-terminated isoimide oligomers and their corresponding imide oligomers have been synthesized by using trifluoroacetic anhydride or acetic anhydride as dehydrating agent, respectively. Their main structure was confirmed by Fourier transform infrared spectroscopy (FTIR). The isoimide oligomers were amorphous and showed excellent solublility in many common solvents, such as acetone and tetrahydeofuran, whereas the imide oligomers cannot dissolve in them. Differential scanning calorimetry and rheometer were used to study crosslinking behavior and processability of these oligomers. The isoimide oligomers exhibited considerably wider processing window and lower viscosity compared with imide ones. As expected, the isoimide form could be converted to imide form through thermal treatment, which could be demonstrated by FTIR. After the oligomers were cured, the polyisoimides showed similar properties compared with corresponding polyimides. © 2011 Wiley Periodicals, Inc. J Appl Polym Sci 122: 3493–3503, 2011

Key words: polyisoimides; polyimides; processability; thermal properties; structure–property relations

INTRODUCTION

Thermosetting polyimides are indispensable in various high-technology areas, such as in modern aerospace and aviation industry, advanced insulator, dielectric manufacturing and packaging technology, because of their excellent electrical, thermal, and high temperature mechanical properties,[1–5] accordingly, many polyimide materials have found wide spread commercial use as coating resins, adhesives, films, foams, and composite matrices.[3,6–11] The imide oligomers, however, are often of poor solubility and fusibility partly due to aromatic heterocyclic structure and the strong interchain interaction, which seriously affects the processability.[3,7,9,12]

Lots of efforts have been devoted to improve the processability of polyimides while maintaining their excellent properties, to circumvent those limitations mentioned-above.[13–18] Initially, soluble precursor such as poly(amic acid)s were utilized for fabrication via thermal imidization; but this method may bring defects in chemical structure and usually need high pressure during processing, which limits the applications of polyimides in high-precision devices.[19] Therefore, soluble polyimides would be desirable instead of precursors. From the synthetic chemistry point of view, structural modifications of the polymer backbone have been developed to realize the improvement of solubility, such as the introduction of flexible links (e.g., O, S, CO, SO_2, and CH_2), bulky lateral substituents (fluorenylidene, hexafluoropropylidene, etc.),[8,20,21] heterocyclic groups,[22–24] as well as copolymerization with other monomers and designation of asymmetric monomers, such as polyimides from isomeric dianhydride.[25–30] Some of these modifications may also have good effects on improving melt processability of imide oligomers. Besides, phenylethynyl-endcapped oligoimides have been attractive in recent years,[31–34] because of relatively large processing window between the melting temperature and the crosslinking temperature. Some phenylethynyl-terminated polyimide matrix resins with low melt viscosity for Resin Transfer Molding process have been developed. However, the curing temperature of those polyimides is more than 350°C, which could cause high cost and disadvantage when processing.

Correspondence to: Z. Wang (wangzhen@ciac.jl.cn) and T. Zhao (tzhao@iccas.ac.cn).

It is essential to reduce the melting point and improve the solubility of imide oligomers as much as possible. Polyisoimides were considered as potential precursors for polyimides. A class of isoimide oligomers, which had lower melting point and wider solubility range than analogous imide oligomers, were claimed in some patents.[35–38] Among all the oligomers, an acetylene-terminated isoimide oligomer was known by the trade name Thermid IP-600,[39,40] whereas its properties have been rarely published in articles. Landis[41] also developed a copolymer formed from a reactive functional terminal isoimide oligomer and another compound, to provide liquid blend on heating and then to cure. Later on, lots of works were concentrated on the isomerization and cure behavior of isoimide oligomers using different methods, such as Fourier transform infrared (FTIR),[39,40] differential scanning calorimetry (DSC),[42] carbon-13 magic-angle spinning Nuclear Magnetic Resonance (^{13}C NMR),[42,43] and nitrogen-15 solid-state Nuclear Magnetic Resonance (^{15}N NMR).[44] Furthermore, Kurita et al.[2] have studied the structural influence on the properties of model isoimides and facile synthesis of polyisoimides in details. Mochizuki and Ueda et al.[45,46] have developed a new photosensitive polyimide precursor based on polyisoimide. However, the properties of thermoset polyisoimide as composite matrix, especially the potentially good processability of isoimide oligomers, have not drawn so much attention. Hence, it will make sense to investigate the effect of the chemical structures of isoimide oligomers on their melt processability, thermal stabilities, and mechanical properties.

In this study, we described the development of novel low-molecular weight isoimide oligomers and imide oligomers from 2,3,3′,4′-biphenyl tetracarboxylic dianhydride (3,4′-BPDA), diamines, and 3-aminophenyl acetylene. The differences in their properties including solubility, rheological behavior, thermal properties, and mechanical properties as well as structure–property relationship were discussed. The isoimide oligomers had better processability, and the cured polyisoimides had comparably thermal and mechanical properties with corresponding polyimides.

EXPERIMENTAL

Materials

3,4′-BPDA was synthesized in our lab. 4,4′-Oxydianiline (4,4′-ODA) and 3,4′-oxydianiline (3,4′-ODA) were purchased from Changzhou Sunchem Electronic Material, China. 3-Aminophenyl acetylene was commercially available from Shandong Jiaozhou Fine Chemicals, China, and was purified by distillation under reduced pressure before use. Triethylamine was used after distillation in the presence of phthalic anhydride and then calcium hydride. *N*,*N*-Dimethylacetamide (DMAc) was purified by distillation over phosphorus pentoxide under reduced pressure and stored over 4 Å molecular sieves. Trifluoroacetic anhydride (TFAA) was purchased from Shanghai Bangcheng Fine Chemicals, China, and used as received without further purification. All the other reagents were purchased from Beijing Beihua Fine Chemicals, China.

Synthesis

Preparation of acetylene-terminated isoimide oligomers based on 3,4′-BPDA and 3,4′-ODA (m-AII) or 4,4′-ODA (p-AII)

A three-necked 500 mL round bottom flask was fitted with a thermal meter, magnetic stirrer, nitrogen inlet and outlet. The flask was charged with 3,4′-BPDA (9.408 g and 0.032 mol) and DMAc (90 mL). After 3,4′-BPDA dissolved in the stirring solution completely, 3,4′-ODA (3.2 g and 0.016 mol) dissolved in DMAc (60 mL) was added dropwise over a 10–20 min period. Then the reaction mixture was stirred for 2 h under nitrogen and a solution of 3-aminophenyl acetylene (3.744 g and 0.032 mol) dissolved in DMAc (60 mL) was added. After the addition of the 3-aminophenyl acetylene, the solution was stirred for an additional 6 h at room temperature, and TFAA (26.88 g and 0.128 mol) was added dropwisely, maintaining the temperature in the range of 10–25°C by means of an ice bath. The reaction mixture was maintained at room temperature for approximately 12 h. The oligomer was then precipitated by pouring the reaction mixture into 800 mL water and washed thoroughly with fresh water till the PH value of the filtrate was about 7.

The resultant precipitate was dried under vacuum at 90°C for several hours to afford bright yellow powder (yield: 14.36 g, 94%).

Acetylene-terminated isoimide oligomer based on 3,4′-BPDA and 4,4′-ODA (*p*-AII) can be prepared according to the same procedure. The oligomer of *p*-AII was also bright yellow powder.

Preparation of acetylene-terminated imide oligomers based on 3,4′-BPDA and 3,4′-ODA (m-AI) or 4,4′-ODA (p-AI)

3,4′-BPDA (9.408 g and 0.032 mol) was dissolved in DMAc (90 mL) in a three-necked 500 mL round bottom flask equipped with a thermal meter, magnetic stirrer, nitrogen inlet and outlet. After stirring at room temperature for 15 min, a clear solution was obtained. 3,4′-ODA (3.200 g and 0.016 mol) was added incrementally to the solution, and the reaction

was allowed to proceed for 2 h at room temperature under nitrogen atmosphere. To the synthesized polyamic acid solution, 3-aminophenyl acetylene (3.744 g and 0.032 mol) was added and allowed to react for an additional 6 h to end-cap the acid anhydride end-groups of polyamic acid. Then acetic anhydride (16.640 g and 0.128 mol) and triethylamine (5.547 g and 0.055 mol) were added one by one with stirring, and the reaction mixture was stirred for about 12 h at room temperature. Finally, the solution was poured into a large excess amount of water. The precipitate was filtered off, washed with fresh water for 3 times, and ethanol for one time.

The product designated *m*-AI was dried under vacuum at 90°C for several hours to afford light gray powder (yield: 14.05 g, 92%).

Acetylene-terminated imide oligomer based on 3,4′-BPDA and 4,4′-ODA (*p*-AI) could be obtained following the same procedure noted earlier if only 4,4′-ODA was charged instead of 3,4′-ODA. The oligomer of *p*-AI was bright yellow powder.

Preparation of the cured polyimide and polyisoimide resins and the composites composed of the cured polyimide and polyisoimide resins and glass cloth

The cured polyimide and polyisoimide resins were obtained by curing those oligomers in the following heating profile: 170°C for 3 h, 200°C for 1 h, 230°C for 1 h, and 250°C for 3 h in an oven open to the air.

The preparation procedure of composite is described as follows: An oligomer was dissolved in suitable solvent, e.g., *m*-AI in dimethylformamide (DMF) or *m*-AII in acetone. Glass cloth was dipped into the solution and then vertically hung. The solvent was allowed to evaporate at certain temperature. The samples were cured in a closed steel mold at a high pressure by the following heating profile: 170°C for 3 h, 200°C for 1 h, 230°C for 1 h, and 250°C for 3 h. Then the composite sheet will be cut into fit size for DMA testing. The weight percentage of the resin in the final composites was determined to be 35–40% by calculating the difference between the weights of the bare glass cloth and the composites.

Characterization

FTIR spectrum was recorded on a Bruker 27 IR spectrometer with KBr disks for solid samples. ^{1}H NMR spectra were recorded in dimethyl sulfoxide-d_4 solvent with a Bruker AV400 spectrometer. The molecular weight of the oligomers sample was determined by gel permeation chromatography (GPC) with tetrahydrofuran (THF) as the eluant (1.0 mL/min) at 35°C using a Waters 1500 system. The spectrum was calibrated with narrow polystyrene standards. Wide angle X-ray diffraction (XRD) was conducted on a Rigaku D/max-2500 X-ray diffractometer with Cu/K a1 radiation, operated at 40 kV and 200 mA. Thermal behavior was analyzed with a Mettler Toledo 822e instrument DSC using a heating rate of 10°C/min in a nitrogen atmosphere. Thermogravimetric analysis was performed on a Netzsch STA 409PC instrument with ramping rate of 10°C/min under nitrogen or air at a flow rate of 50 mL/min. Dynamic mechanical analysis (DMA) was performed on a DMA 242 C (NETZSCH, Germany) with a driving frequency of 1.0 Hz, single cantilever mode and a scanning rate of 5°C/min in nitrogen. The size of the composites for DMA measurement was 20 mm × 8 mm × 2 mm. Melt viscosity measurements was performed on a AR2000ex spectrometer (USA) at a ramp rate of 4°C/min in air and the top parallel plate was oscillated at a fixed strain of 10% and a fixed angular frequency of 100 rad/s. Sample specimen discs of 2.5 cm diameter and 1 mm thickness were prepared by press molding oligomer powder at room temperature under high pressure. The microstructure morphology of the surface of resin was explored by means of scanning electron microscope (SEM, Hitachi *S*-4800, Japan).

RESULTS AND DISCUSSION

Synthesis and characterization of the imide and isoimide oligomers

The isoimide oligomers (*m*-AII and *p*-AII) and imide oligomers (*m*-AI and *p*-AI) were all designed with calculated number average molecular weight of 951 g/mol. The synthetic routes were illustrated in Scheme 1. The FTIR spectra unambiguously supported the structures of the oligomers as illustrated in Figure 1. The strong band at 1796 cm^{-1} was characteristic of the C═O in isoimide ring, and the strong one at 933 cm^{-1} was ascribable to the C—O—C in isoimide ring in *m*-AII and *p*-AII spectra. For the *m*-AI and *p*-AI, the bands present at 1777 and 1726 cm^{-1} were due to the symmetric stretch and the asymmetric stretch of the imide carbonyl C═O, respectively. Furthermore, characteristic C—N—C band in imide ring was strong at 1376 cm^{-1} for imide oligomers, but too weak to find out in *m*-AII and *p*-AII spectra. Besides, the very weak peak at 2107 cm^{-1} was assigned to the stretching vibrations of ethynyl group (C≡C).

Figure 2 showed the ^{1}H NMR spectrum of a representative isoimide oligomer (*m*-AII) in dimethylsulfoxide (DMSO)-d6 as solvent. All of the protons in the acetylene-terminated isoimide oligomer as expected were detected. It needs to be emphasized

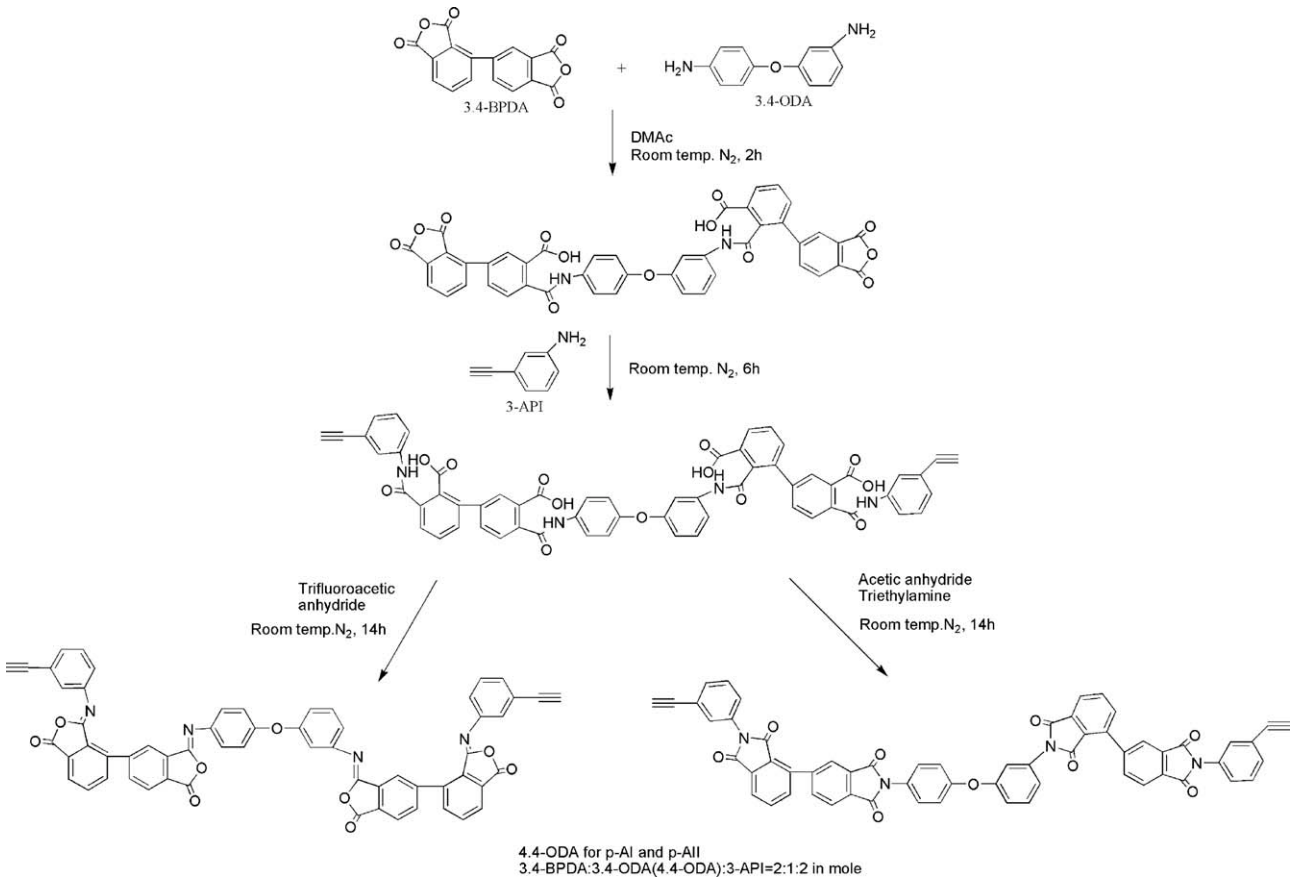

Scheme 1 Synthetic routes of isoimide and imide oligomers.

that there were peaks assigned to —OH and —NH— protons in the region of 13.1–13.3 and 10.5–11.3 ppm as shown in Figure 2, which was due to the uncyclization of the five-ring in isoimide structure. Under the assumption that all the reagents could be utilized in the molecular synthesis, the uncyclization rate in the structure of isoimide oligomer could be calculated according to the equation as follows:

$$R = (\mathrm{Ph} \times 28n)/(B \times 4n) \quad (1)$$

where R is the uncyclization rate, Ph is the integrated intensity of hydrogen in —OH group, B is the integrated intensity of hydrogen on the benzene ring, and n is the mole of diamine used in preparation.

Because the hydrogen in —OH group is active hydrogen, Ph has deviation to some degree. R was calculated as 14%.

Figure 3 showed typical GPC curves of the isoimide and imide oligomers (*m*-AII and *m*-AI), in which it could be seen that each of them was a complex resin mixture consisted of several resin species with different molecular weights. Oligomers of thermosetting polyimides usually have molecular distribution with the designed molecular weight monomer as the chief component.[26,47,48] Herein, all the designed molecular weight for oligomers was 951 g/mol (viz. repeat unit $n = 1$). Oligomers *m*-AII and *m*-AI nearly had the same molecular distribution as shown in Figure 3 with the $n = 1$ component as the largest. For *m*-AII and *m*-AI, the number molecular weight determined by GPC was Mn of 932 and 945, respectively, in well accordance with the

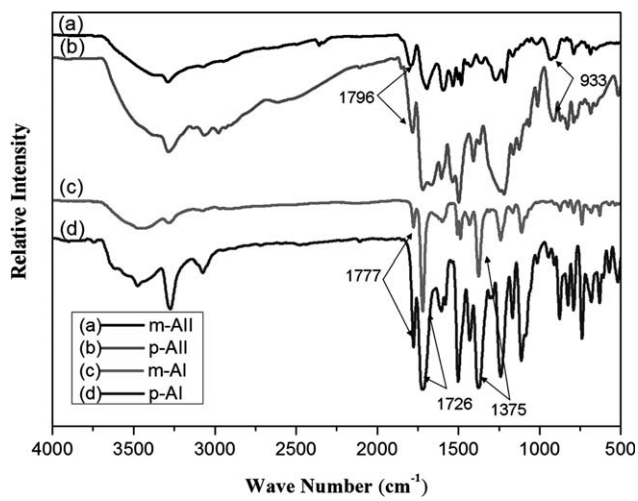

Figure 1 The FT-IR spectra of isoimide and imide oligomers.

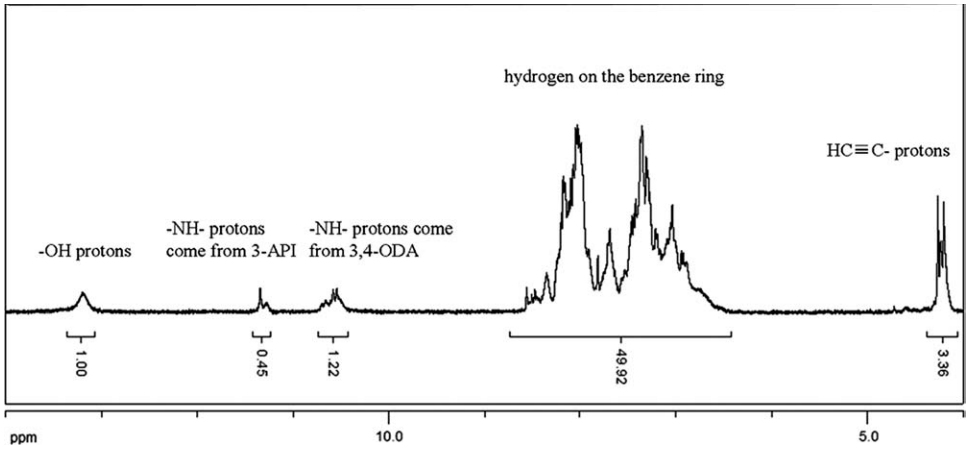

Figure 2 The ^{1}H NMR spectrum of a representative isoimide oligomer (*m*-AII).

calculated Mn of 951. Because *p*-AI did not dissolve in THF, the GPC curve of *p*-AI and *p*-AII was not collected in Figure 3.

Processability of the imide and isoimide oligomers

The solubility of all the four oligomers was summarized in Table I. In general, all the four oligomers were soluble in polar aprotic solvents, such as DMF, DMAc, and n-methylpyrrolidone. P-AI could not be dissolved in THF, whereas *m*-AI could be done due to its whole isomeric structure, whose twisty chain probably inhibits interchain interaction and chain packing.[49] It was gratifying to find that isoimide oligomers showed much higher solubility in sharp contrast to imide oligomers. As shown in Table I, *m*-AII and *p*-AII were resolvable in acetone, however, *m*-AI and *p*-AI were not. The reason may be owing to the coaction of the isomeric and the isoimide structure. The isoimide oligomers will be more suitable for conventional molding or dipping techniques.

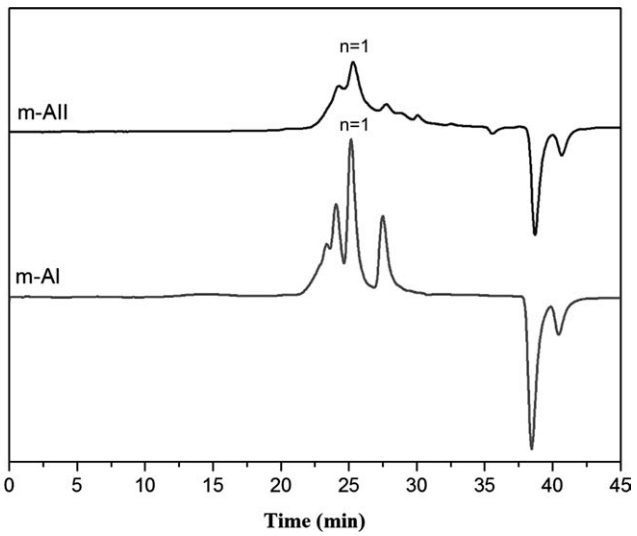

Figure 3 The GPC curves of *m*-AI and *m*-AII.

X-ray diffractionmetry could also illustrate the reason why isoimide-structure oligomers have excellent solubility. Figure 4 depicted the XRD curves of the four oligomers, in which it can be seen that *m*-AII and *p*-AII were amorphous according to the "bread peaks" between 10°and 30°. It was assumed that the isoimide structure in the backbone had effect of reducing the chain-to-chain interaction and packing efficiency, resulting in the reduction of crystallinity. In addition, *m*-AI and *p*-AI have some crystal phase from the relatively sharp peaks at the region of 10–30°despite the effect of the asymmetry of 3,4-BPDA, which may be due to the crystal content of AI-n0 (as shown in Fig. 4) in the mixture of *m*-AI and *p*-AI. AI-n0 (repeat unit $n = 0$) was one component in *m*-AI as shown in GPC curve of Figure 3 and was demonstrated to have crystal phase by XRD in Figure 4. The same phenomenon could be seen for other low-molecular weight polyimide oligomers.[47,50,51] After *m*-AI and *p*-AI were cured, *m*-API (cured *m*-AI) and *p*-API (cured *p*-AI) were amorphous as shown in Figure 4.

Rheometer was used to investigate meltability of oligomers. As shown in Figure 5, although *m*-AI was based on isomeric dianhydride and diamine, the viscosity of it did not decrease as the temperature increased in the melting range tested by DSC

TABLE I
The Solubility of Oligomers in Different Solvents

	Acetone	THF	DMF	DMAc	DMSO	NMP
m-AII	++	++	++	++	++	++
p-AII	+	++	++	++	++	++
m-AI	−−	++	++	++	++	++
p-AI	−−	−−	++	++	++	++

++ = soluble; + = soluble under heating; −− = insoluble.

THF = tetrahydrofuran; DMF = *N*,*N*-dimethylformamide; DMSO = dimethylsulfoxide; NMP = N-methyl-2-pyrrolidinone.

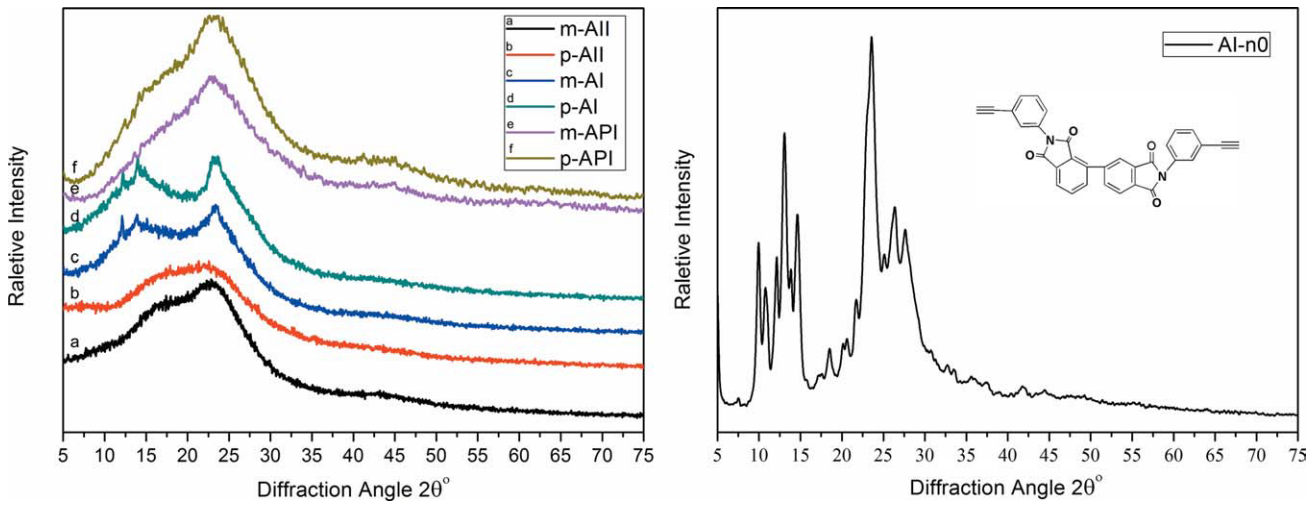

Figure 4 The XRD curves of the oligomers and cured oligomers. [Color figure can be viewed in the online issue, which is available at wileyonlinelibrary.com.]

(mentioned later), but presented up and down regularly. There was one possible reason for this phenomenon that the oligomer was melting meanwhile the crosslinking reaction happened. The viscosity went up quickly after 180°C, so there was narrow processing window for *m*-AI. In contrast to imide oligomer, both *p*-AII and *m*-AII containing isoimide structure in the backbone presented broader processing window and lower viscosity from nearly 175 to 220°C, which meant good meltability. In general, the viscosity decreased when the tendency of melt was dominant and increased when polymerization was in charge. The complex viscosity $|n^*|$ of *p*-AII was below 1000 Pa s in the range of 180–222°C with the minimum 114 Pa s at 201°C. The processing window of *m*-AII was wider than *p*-AII for the reason that isomeric diamine was introduced in its main chain besides isomeric dianhydride. The $|n^*|$ of *m*-AII was below 1000 Pa s between 173 and 226°C and the lowest value was 43 Pa s at 201°C. In summary, not only isomeric but also isoimide structure contributed to the good processability, especially the latter. In the view of melt viscosity, acetylene-terminated *m*-AII and *p*-AII had good fluidity to be able to impregnate the reinforced-materials at lower temperature than phenylethynyl-endcapped oligoimides, which cured on 350°C or higher.[26,47]

Cure behavior of oligomers and demonstration of isoimide–imide transformation

Thermal behaviors of all the four acetylene-functional oligomers were examined by DSC. Figure 6 showed the DSC thermograms of *m*-AII and *p*-AII in comparison with *m*-AI and *p*-AI. P-AI showed the highest melting temperature range of 170–210°C with the peak at 200°C. M-AI showed somewhat lower range of 160–205°C, which might be due to the more asymmetric

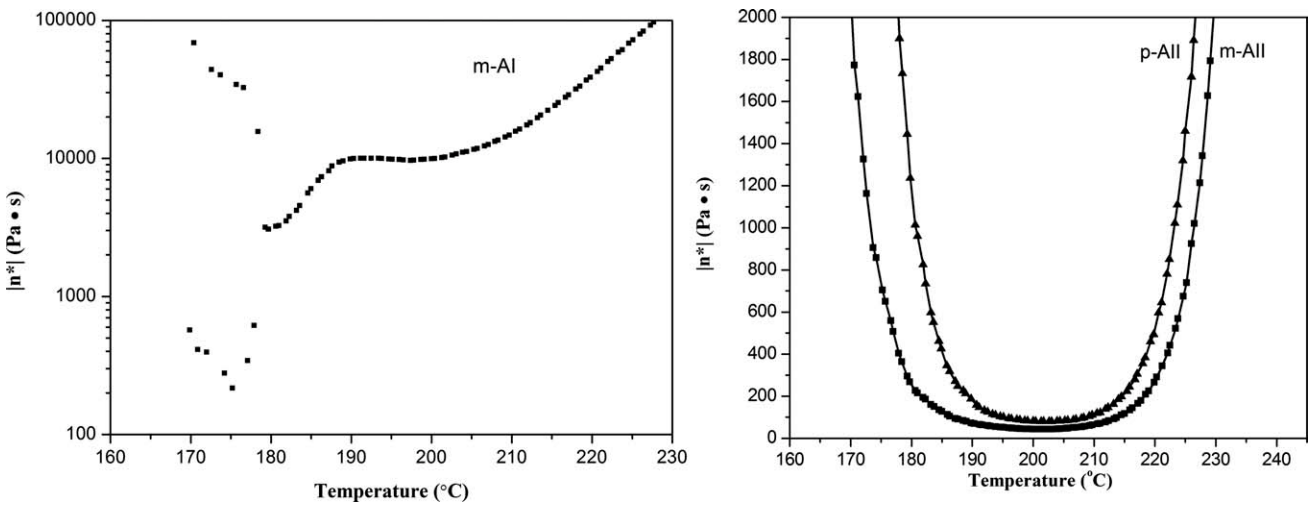

Figure 5 The melt viscosity on temperature for oligomers.

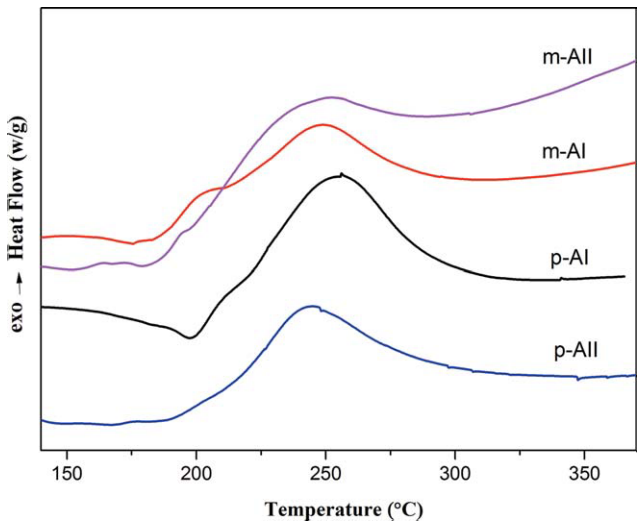

Figure 6 The DSC curves of oligomers. [Color figure can be viewed in the online issue, which is available at wileyonlinelibrary.com.]

molecular structure based on isomeric dianhydride and diamine. However, there was no evidence for melting endotherms in DSC trace for oligomer *m*-AII and *p*-AII. The reason may be that the exothermic isoimide–imide conversion spaned this temperature, masking the melting endotherm.[40]

The addition cured reaction of *m*-AI and *p*-AI showed an exothermic peak initializing at about 210°C with a maximum at about 260°C. The onset temperature of exothermic peak for *m*-AII and *p*-AII was 10–20°C lower than *m*-AI and *p*-AI, which may be owing to the conversion from isoimide to imide. The maximum and ending temperature of the peaks was the same as imide ones at 250–260°C and 300°C, respectively.

According to the dynamic DSC shown in Figure 6, the onset of the addition polymerization was about 210°C with ending at around 300°C. The isoimide–imide conversion could not be recognized from DSC clearly. Some researchers studied the conversion using FTIR in detail and concluded that the rearrangement started before curing and slowed down due to the curing three-dimensional structure.[39,40] So the curing procedure listed in the section of synthesis was chosen with extension of the time at 170 and 250°C for fully converting and curing.

FTIR method was used to track the isoimide–imide converting and crosslinking reaction of acetylene group following the cure procedure mentioned before. The profiles of FTIR spectra for *m*-AII with different curing temperature and increase in curing time were depicted in Figure 7. The FTIR spectra of the unreacted *m*-AII showed the characteristic band of isoimide structure towards 1796 and 933 cm^{-1}, and the characteristic band of acetylene group towards 2107 cm^{-1}, all of which remained after treating at 100°C for 15 min. From 170 to 250°C in cure procedure, it was remarkable that the intensity of the bands for isoimide structure decreased to considerable extent with the proceeding of the isoimide–imide transformation. Meanwhile the band at 1777, 1726, and 1376 cm^{-1}, characteristic for imide structure, formed at 170°C and increased as the converting reaction progressed. These indicated that the isoimide–imide converting reaction happened at about 170°C and almost completed at the ending of cure procedure. The weak absorption at 2107 cm^{-1} started to decrease after the sample was treated at 200°C for 1 h and disappeared when the cure procedure ended at 250°C for 3 h. This implied that there was no acetylene group in the final crosslinking network for polyisoimide (*m*-AIPI). Unexpectedly, however, the characteristic infrared C=O absorption at 1850 cm^{-1}

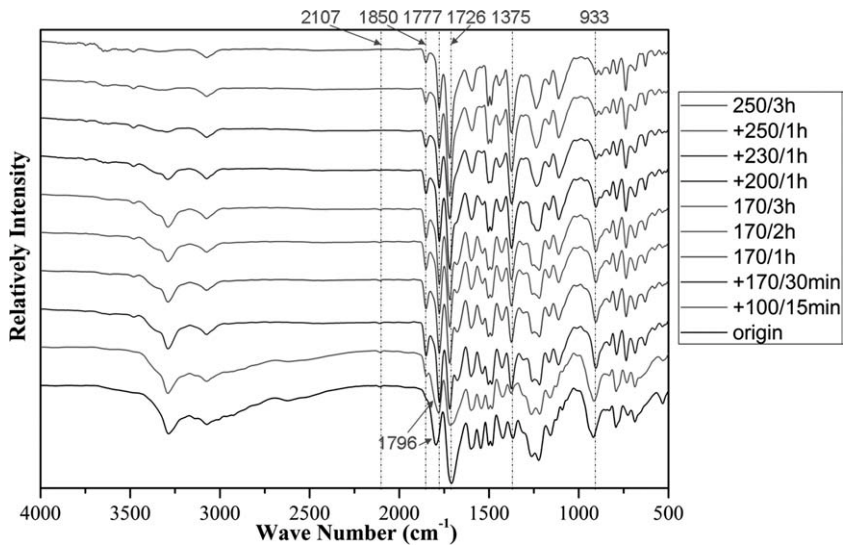

Figure 7 The FT-IR spectra for *m*-AII with different curing temperature and increase in curing time. [Color figure can be viewed in the online issue, which is available at wileyonlinelibrary.com.]

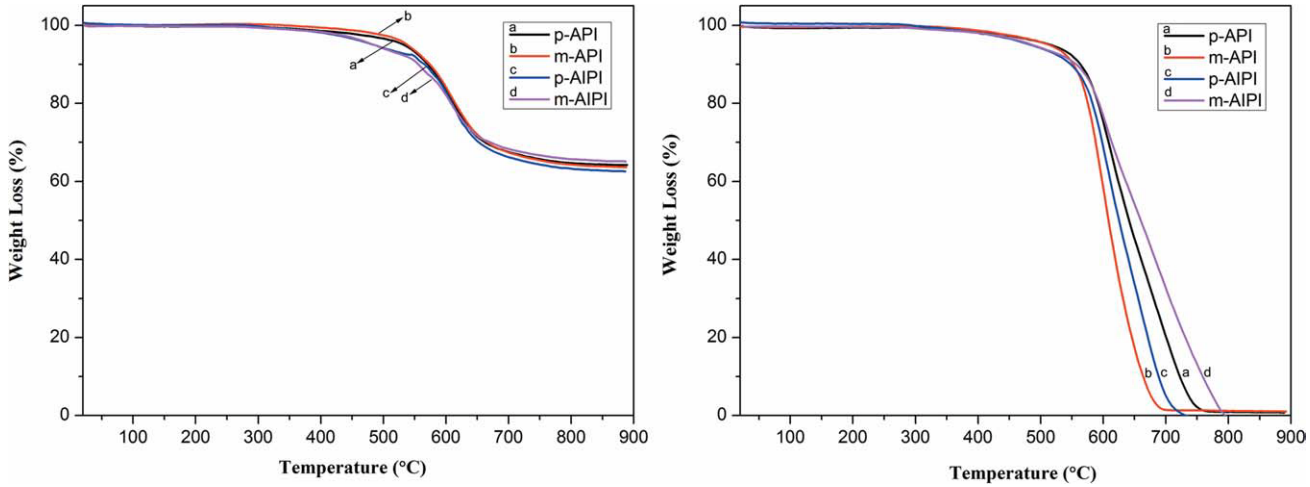

Figure 8 The TGA curves of cured oligomers in nitrogen and air. [Color figure can be viewed in the online issue, which is available at wileyonlinelibrary.com.]

appeared after 170°C, which was attributed to the formation of anhydride structure by the dehydration of uncyclizated ring intermolecularly under heat treatment. The reason of dehydration was that, as mentioned in the section of synthesis and characterization of the imide and isoimide oligomers, there was little amount of uncyclizated five-ring in isoimide monomer structure.

Thermal properties of the cured polyimide and polyisoimide resins

All the four oligomers *m*-AII, *p*-AII, *m*-AI, and *p*-AI can be thermally cured to polyisoimide (named *m*-AIPI and *p*-AIPI) and polyimide (named *m*-API and *p*-API). The thermal and thermo-oxidative stability of *m*-AIPI, *p*-AIPI, *m*-API, and *p*-API were investigated by TGA under nitrogen and air atmosphere. The thermograms were shown in Figure 8, and the data were collected in Table II. All the four polymers showed high temperature of 5% and 10% weight loss not only in nitrogen but also in air, which revealed high thermal and thermo-oxidative stability, even though cured polyisoimides (*m*-AIPI and *p*-AIPI) were a little less stable in comparison with cured polyimides (*m*-API and *p*-API). In addition, *p*-API and *p*-AIPI, using 4,4′-ODA as reagent, presented a little more stable than corresponding *m*-API and *m*-AIPI based on 3,4′-ODA. This phenomenon was the same as some articles described before.[52] Char yield of polyimides and polyisoimides at 900°C were all over 60%.

Dynamic mechanical properties of the composites based on the cured polyimide and polyisoimide resins

DMA was used to study the dynamic mechanical properties of composites derived from the cured polyimide and polyisoimide resins and glass cloth. The composites were prepared as mentioned in the section of synthesis.

The glass transition temperatures (T_g) of the composites was defined by the tan δ peak temperature. As shown in Figure 9 and Table II, all polymers showed high T_g around 350°C, whereas the final cure temperature in curing procedure was 250°C. It meant that these composites with low curing

TABLE II
Thermal Property Data of the Cured Resins

		5% weight loss (°C)		10% weight loss (°C)		Char yield (%)[b]	
Cured resins	T_g (°C)[a]	In N_2	In air	In N_2	In air	In N_2	In air
p-API	–[c]	553	516	582	560	67	0
m-API	350	546	513	578	552	67	0
p-AIPI	371	485	475	566	550	63	0
m-AIPI	357	482	471	556	551	65	0

[a] The glass transition temperature determined from DMA.
[b] Char yield at 900°C determined from the TGA analysis.
[c] Not measured due to the difficulty of composite preparing.

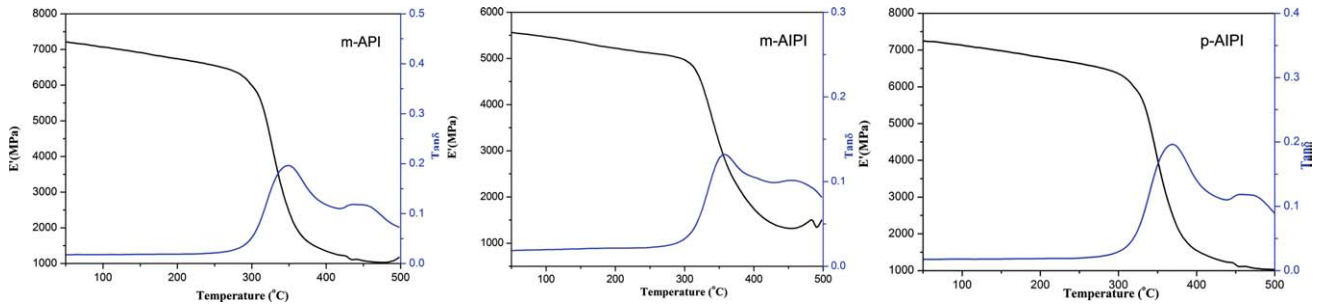

Figure 9 DMA curves of composites derived from the cured resins and glass cloth. [Color figure can be viewed in the online issue, which is available at wileyonlinelibrary.com.]

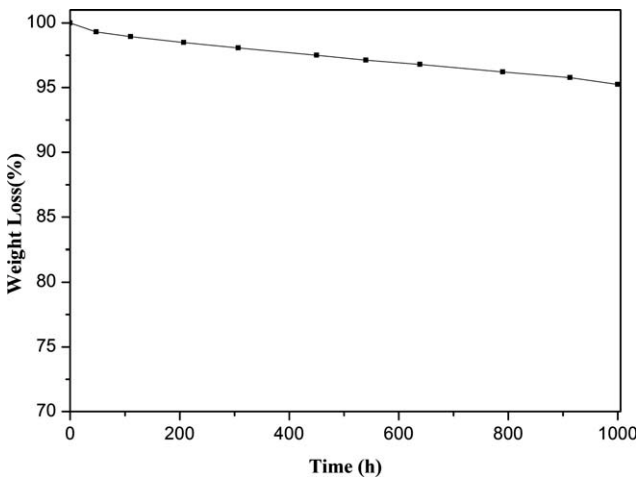

Figure 10 The thermal oxidative aging curve of *m*-AIPI at 300°C for 1000 h.

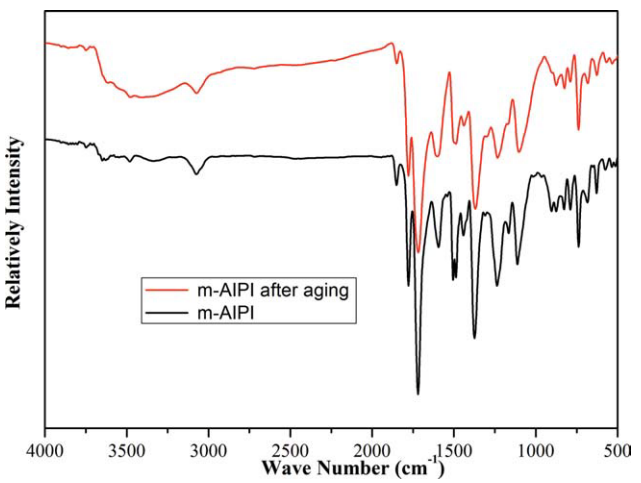

Figure 11 The FT-IR spectra of *m*-AIPI before and after aging at 300°C. [Color figure can be viewed in the online issue, which is available at wileyonlinelibrary.com.]

temperature could be used in high-temperature conditions. Furthermore, *m*-API and *m*-AIPI should have nearly the same structure after the *m*-AIPI's conversion from isoimide to imide on heating treatment. Interestingly, the T_g of *m*-AIPI was a little higher than *m*-API's. The reason can be explained by the formation of anhydride from dehydration intermolecularly as mentioned in the section of synthesis and characterization in Results and Discussion, which brought larger crosslinking density and higher T_g. For the phenomenon that T_g of *p*-AIPI was a little higher comparing with *m*-API and *m*-AIPI, the influencing factor was presumably the rigidness of the reagent structure. The *para*-position of 4,4′-ODA may be of better rigidness than *meta*-position.[52]

Thermal oxidative aging property of polyisoimide

m-AIPI was taken as example to investigate the thermal oxidative aging property of polyisoimide, due to its good processability and dynamic

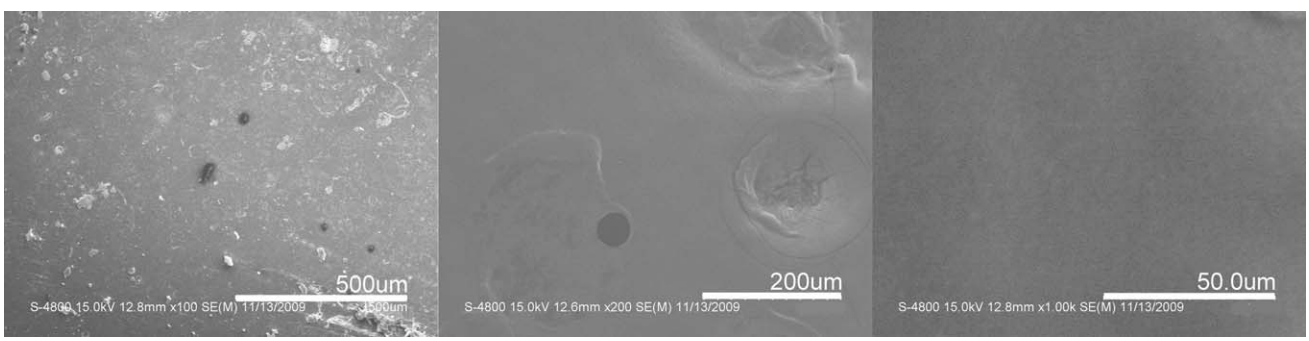

Figure 12 The microstructure morphology of the aging sample surface by SEM.

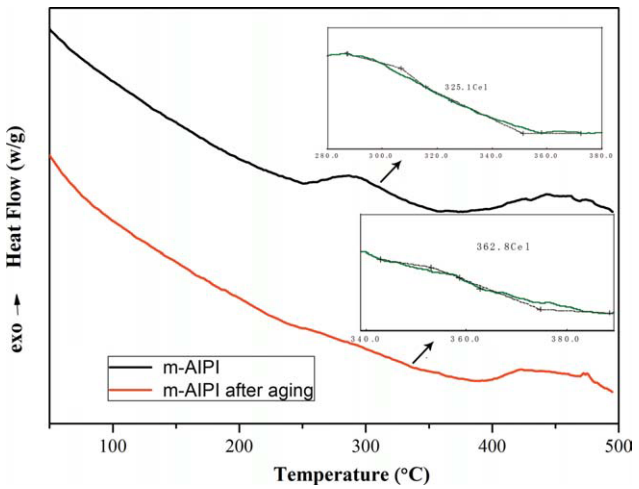

Figure 13 The DSC curves of *m*-AIPI before and after aging at 300°C. [Color figure can be viewed in the online issue, which is available at wileyonlinelibrary.com.]

mechanical property. The pure cured resin with the size of 1 cm × 1 cm × 0.4 cm was tested in air atmosphere aging oven at 300°C for 1000 h and weighted at interval of 100 h approximately. The curve of weight versus time was shown in Figure 10. The data were calculated by the average value of three parallel samples. After 1000 h aging at 300°C in atmosphere of air, the samples were still thickening cuboid state, and the average weight loss was 4.58% (<5%), which meant that little structure was oxidated and little fragment left from the cured resin system, revealing excellent thermo-oxidative stability. The surface part of the aged *m*-AIPI (the most easily oxidated portion of the resin cuboid) was investigated compared with the sample before aging by FTIR. As shown in Figure 11, nearly no peak changed before and after aging except the formation of —OH group in the aged resin. The aromatic ether structure in 3,4′-ODA may be the weak part under thermal-oxidative condition, resulting in leave of the benzene derivatives and formation of -OH group.[53]

The microstructure morphology of the sample surface was explored by SEM, as shown in Figure 12. After 1000 h aging, there was no large fracture on the surface, but only some small subsidence damage with size of 100 μm diameter nearly. The phenomena anastomosed with the little weigh loss after aging, which could also support evidence for good thermo-oxidative ability of polyisoimide (*m*-AIPI). Furthermore, because of the micro crack and brittleness of resin casting body, DMA was not suitable to test the difference of T_g before and after aging. Alternatively, DSC was used. As we known, the T_g tested by DSC was different from the one by DMA, however, same testing method could illustrate the change on T_g. As shown in Figure 13, the T_g of *m*-AIPI before aging was 325°C, 30°C lower than the one tested by DMA. After aging, the T_g did not appear clearly and was measured as 362°C. On one hand, the aging condition made oxidation on the cured resin, and on the other hand it postcured the resin and enhanced the T_g of polymer, especially when the cured resin had excellent thermal-oxidative property.

CONCLUSIONS

Novel low-molecular weight isoimide oligomers based on isomeric dianhydrides, diamines, and 3-aminophenyl acetylene were successfully synthesized. As a result of introduction of isoimide structure, isoimide oligomers possessed better solubility and lower viscosity than corresponding imide ones. Rheometer study showed a "processing window" between 175 and 225°C with the complex viscosity $|n^*|$ below 1000 Pa s and the lowest near 50 Pa s. As cure procedure proceeded, both the isoimide–imide converting and crosslinking reaction underwent, which was illustrated by FTIR. The cured polyisoimides demonstrated higher glass transition temperature and comparative thermal stability in comparison with analogous imide oligomers. In addition, polyisoimides possessed excellent thermo-oxidative stability with <5% weight loss at 300°C for 1000 h. These indicated that the isoimide oligomers developed in this article had potential to be used as low-temperature curing but high-temperature using matrix resin.

The authors express their thanks to the National 973 Project of China (No. 2010CB631100) and Jilin Province Science and Technology Development Projects (No. 20080110) for their financial supports.

References

1. Ding, M. Prog Polym Sci 2007, 623.
2. Kurita, K.; Suzuki, Y.; Enari, T.; Ishii S.; Nishimura, S.-I. Macromolecules 1995, 28, 1801.
3. Feger, C.; Franke, H. Polyimides: Fundamentals and Applications; Marcel Dekker: New York, 1996.
4. Wilson, D. Progress in Polyimides; Chapman and Hall: New York, 1990.
5. Ishii, J.; Takata, A.; Oami, Y.; Yokota, R.; Vladimirov, L.; Hasegawa, M. Eur Polym J 2010, 46, 681.
6. Hergenrother, P. M.; Watson, K. A.; Smith J. G., Jr.; Connell, J. W.; Yokota, R. Polymer 2002, 43, 5077.
7. Sroog, C. E. Prog Polym Sci 1991, 16, 561.
8. Hergenrother, P. M. High Perform Polym 2003, 15, 3.
9. Wilson, D.; Stenzenberger, H. D.; Hergenrother, P. M. Polyimides-Chemistry and Application; Blackie and Sons Ltd.: New York, 1990.
10. Yu, X. H.; Zhao, X. G.; Liu, C. W.; Rai, Z. W.; Wang, D. M.; Dang, G. D.; Zhou, H. W.; Chen, C. H. J Polym Sci A Polym Chem 2010, 48, 2878.
11. Liu, X. Y.; Zhan, M. S.; Shen, Y. X.; Wang, K. J Appl Polym Sci 2011, 119, 3253.

12. Yan, J.; Wang, Z.; Gao, L.; Ding, M. Polymer 2005, 46, 7678.
13. Korshak, V. V.; Vinogradova, S. V.; Vygodskii, Y. S. J Macromol Sci C Polym Rev 1974, 11, 45.
14. Husk, G. R.; Cassidy, P. E.; Gebert, K. L. Macromolecules 1988, 21, 1234.
15. Matsuura, T.; Ishizawa, M.; Hasuda, Y.; Nishi, S. Macromolecules 1992, 25, 3540.
16. Spiliopoulos, I. K.; Mikroyannidis, J. A. Macromolecules 1996, 29, 5313.
17. Grubb, T. L.; Ulery, V. L.; Smith, T. J.; Tullos, G. L.; Yagci, H.; Mathias, L. J.; Langsam, M. Polymer 1999, 40, 4279.
18. Chung, I. S.; Kim, S. Y. Macromolecules 2000, 33, 3190.
19. Rozhanskii, I.; Okuyama, K.; Goto, K. Polymer 2000, 41, 7057.
20. Serafini, T. T.; Delvigs, P.; Lightsey, G. R. J Appl Polym Sci 1972, 16, 905.
21. Zuo, H.; Chen, J.; Hu, A.; Fan, L.; Yang, S. Eur Polym J 2007, 43, 3892.
22. Vannucci, R. D. SAMPE Q 1987, 19, 31.
23. Wilson, D. Br Polymer J 1988, 20, 405.
24. Scola, D. A.; Vontell, J H. Polym Eng Sci 1991, 31, 6.
25. Bryant, R. G.; Jensen, B. J.; Hergenrother, P. M. Polym Prepr 1993, 34.
26. Hergenrother, P. M.; Bryant, R. G.; Jensen, B. J.; Havens, S. J. J Polym Sci A Polym Chem 1994, 32, 3061.
27. Hergenrother, P. M.; Smith, J G., Jr. Polymer 1994, 35, 4857.
28. Hasegawa, M.; Sensui, N.; Shindo, Y.; Yokota, R. Macromolecules 1998, 32, 387.
29. Sensui, N.; Ishii, J.; Takata, A.; Oami, Y.; Hasegawa, M.; Yokota, R. High Perform Polym 2009, 21, 709.
30. Ghaemy, M.; Alizadeh, R. Hashemi Nasr, F. J Appl Polym Sci 2010, 118, 3407.
31. Liu, Y.; Wang, Z.; Yang, H.; Gao, L.; Li. G.; Ding, M. J Polym Sci A Polym Chem 2008, 46, 4227.
32. Li, Y.; Morgan, R. J. J Appl Polym Sci 2006, 101, 4446.
33. Zuo, H. J.; Chen, J. S.; Yang, H. X.; Hu, A. J.; Fan, L.; Yang, S. Y. J Appl Polym Sci 2008, 107, 755.
34. Bryant, R. G.; Jensen, B. J.; Hergenrother, P. M. J Appl Polym Sci 1996, 59, 1249.
35. Landis, A. L. Hughes Aircraft Co. (Huga), 1983; p 71372-B.
36. Landis, A. L. Hughes Aircraft Co., 1984.
37. Landis, A. L. Hughes Aircraft Co., 1985.
38. Landis, A. L. Hughes Aircraft Co., 1985.
39. Huang, W. X.; Wunder, S. L. J Polym Sci B Polym Phys 1994, 32, 2005.
40. Huang, W. X.; Wunder, S. L. J Appl Polym Sci 1996, 59, 511.
41. Landis, A.; Naselow, A. Hughes Aircraft Co (Huga) 1985.
42. Kim, Y. J.; Son, G. I.; Kim, J.-H. Polym Int 2002, 51, 379.
43. Swanson, S. A.; Fleming, W. W.; Hofer, D. C. Macromolecules 1992, 25, 582.
44. Murphy, P. D.; Di Pietro, R. A.; Lund, C. J.; Weber, W. D. Macromolecules 1994, 27, 279.
45. Mochizuki, A.; Teranishi, T.; Ueda, M. Macromolecules 1995, 28, 365.
46. Seino, H.; Haba, O.; Ueda, M.; Mochizuki, A. Polymer 1999, 40, 551.
47. Chen, J.; Qu, X.; Liu, J.; Yang, H.; Fan, L.; Yang, S. Polym Eng Sci 2008, 48, 918.
48. Yamaguchi, H.; Aoki, F. J Photopolymer Sci Technol 2006, 19, 269.
49. Li, Q.; Fang, X.; Wang, Z.; Gao, L.; Ding, M. J Polym Sci A Polym Chem 2003, 41, 3249.
50. Li, Y.; Obando, N.; Tschen, F.; Morgan, R. J. J Therm Anal Calorim 2006, 85, 125.
51. Li, Y.; Murphy, L. A.; Lincoln, J. E.; Morgan, R. J. Macromol Mater Eng 2007, 292, 78.
52. Ding, M. X. Polyimide: The Relationship Between Chemistry, Structure and Properties and Materials; Science Press, 2006.
53. Vora, R. H. Mater Sci Eng B 2010, 168, 71.